EES Solar

REVIEW

View Article Online
View Journal | View Issue

Cite this: *EES Sol.*, 2025, **1**, 502

Moving beyond the Shockley–Queisser limit: current bottlenecks and a new direction in solar energy conversion

Mehri Ghasemi, Joel Van Embden, Baohua Jia* and Xiaoming Wen *

Third-generation solar cells offer a promising path to surpass the Shockley–Queisser efficiency limit through innovative materials and architectures. Concepts such as tandem solar cells, hot carrier extraction, carrier multiplication, intermediate band absorption, and photon upconversion each address specific energy loss mechanisms in conventional devices. This review provides a comprehensive overview of major third-generation strategies, outlining their principles, recent progress, and key limitations. Special emphasis is placed on the new conceptual lattice battery solar cell (LBSC), which is able to simultaneously overcome two major energy losses of hot phonon and sub-bandgap non-absorption in conventional solar cells, because LBSC integrates unique energy micro-recycle processes of hot phonon storage and subgap carrier upconversion within a single-junction architecture. Building on this, we introduce the concept of the lattice energy reservoir (LER), a dynamic energy retention mechanism proposed to operate within soft-lattice materials such as metal halide perovskites. LER offers a unified physical basis for LBSC operation by enabling temporal energy storage and reuse through strong lattice–carrier coupling. The LBSC framework highlights a new paradigm in solar energy conversion that leverages intrinsic material properties to overcome efficiency and stability challenges. This review thus aims to guide future efforts toward integrated, high-performance photovoltaic designs grounded in emerging lattice-physics insights.

Received 4th April 2025
Accepted 3rd June 2025

DOI: 10.1039/d5el00053j

rsc.li/EESSolar

Broader context

The development of next-generation solar technologies is vital to achieving carbon neutrality and meeting global energy demands. Conventional single-junction photovoltaic devices are fundamentally limited by intrinsic energy losses such as hot carrier thermalization and sub-bandgap photon transmission, both of which contribute to the Shockley–Queisser limit. Third-generation strategies like tandem solar cells, hot carrier extraction, and upconversion have made progress in addressing these losses, yet face major bottlenecks related to material stability, scalability, and system complexity. This review introduces and consolidates these existing approaches while comparing a new conceptual lattice battery solar cell (LBSC). Unlike traditional strategies requiring ultrafast carrier extraction or complex architectures, LBSC offers a conceptually unified route for capturing and recycling both thermal and sub-bandgap losses within a single absorber material. This shift in paradigm, from immediate energy extraction to temporally stored lattice-mediated energy utilization, may unlock new directions in solar cell design.

1. Introduction

To address future energy requirements and minimize fossil fuel use there has been a global push towards the development of sustainable and renewable energy solutions. Solar energy, noted for its plentiful supply and environmental benefits, already plays a significant role in global electricity generation. Nevertheless, to meet future energy demands and decarbonisation targets, its contribution must grow by orders of magnitude, driving the need for high-efficiency, scalable solar technologies. Solar cells, also known as photovoltaic (PV) cells, harness the photovoltaic effect to transform light into electrical energy. They are among the most environmentally friendly energy sources, alongside options like hydropower and wind energy. Over the last twenty years, advancements in PV technology have continuously improved the power conversion efficiency (PCE) of these solar cells.[1,2] The journey of converting solar energy into electricity through solar cells (SCs) has undergone notable transformations in recent decades. First-generation solar cells, primarily based on crystalline silicon (c-Si), have formed the foundation of the photovoltaic industry for over 70 years. While early devices in the 1950s and 1970s exhibited relatively low efficiencies (around 11%) and high production costs, decades of technological advancements, including improved wafer manufacturing, passivation techniques, and large-scale deployment, have dramatically increased efficiency and

Centre for Atomaterials and Nanomanufacturing, RMIT University, Melbourne, 3000, Australia. E-mail: baohua.jia@rmit.edu.au; xiaoming.wen@rmit.edu.au

reduced costs. Today, c-Si solar cells remain the dominant commercial technology worldwide, with laboratory-scale devices achieving efficiencies approaching 25%, and mass-produced modules exceeding 22%.[1,3] In the quest for highly efficient and cost-effective SCs innovative techniques and materials were introduced, leading to the development of third-generation solar cells. These advanced SCs, which have the potential to exceed the Shockley–Queisser limit, are the focus of this review.

Photovoltaic technologies may be classified by their development stages and the materials utilized.[4] Here is a broad classification: (i) solar cells predominantly based on silicon (Si) and gallium arsenide (GaAs) represent well-established photovoltaic technologies. Silicon, widely used due to its abundance and relatively low manufacturing costs, contrasts with GaAs. Both technologies, however, face challenges such as reduced power conversion efficiencies at elevated temperatures.[5] Although silicon has become more cost-effective over time, the pursuit of alternative materials in second- and third-generation technologies aims not only to lower costs further but also to enhance performance and integration flexibility. (ii) Second-generation devices based on polycrystalline and amorphous thin films were initially introduced with the promise of lower material usage and potentially reduced manufacturing costs compared to crystalline silicon. However, despite these advantages at the module level, crystalline silicon continues to dominate the market due to its higher efficiency, proven reliability, and mature manufacturing ecosystem.[6,7] (iii) Third generation devices utilize solution-processed semiconductor materials, representing an innovative class of photovoltaics aimed at enhancing efficiency and reducing costs. This latest generation include devices made from organics (OPV), natural dyes (DSSC), quantum dots (QD-PV), and halide perovskites (HP-PV).[8,9] According to Green *et al.*[10] third-generation solar cells are characterized by their potential for high power-conversion efficiency combined with low production costs. Considering third-generation solar cells, emerging low-cost photovoltaic materials synthesized through wet chemistry methods have achieved notable efficiencies, reaching approximately 19.2% for organic photovoltaics (OPV) and 26.7% for hybrid perovskite photovoltaics (HP-PV).[11] Further improvements to power conversion efficiencies (PCE) are pivotal not only for meeting the demands of densely populated urban areas constrained by limited space but also for enhancing market competitiveness. However, these advancements are bound by the theoretical limit posited by the Shockley–Queisser (SQ) theory, applicable to all contemporary state-of-the-art solar cell technologies.[12] The SQ limit defines the theoretical maximum efficiency achievable by a single-junction solar cell, determined by evaluating the maximum electrical energy that may be extracted per incident photon. When considering an AM 1.5 solar spectrum, a solar cell equipped with an ideal bandgap absorber (bandgap, $E_g = 1.4$ eV) could theoretically achieve a peak PCE of 33.7%, corresponding to a maximum rated power output of 337 Wp m^{-2} under the standard AM1.5 G solar spectrum. A significant factor contributing to efficiency losses is the mismatch between the broad wavelength distribution of sunlight and the singular bandgap of the cell's active layer. Efficiency losses manifest through five primary loss mechanisms (Fig. 1a and b).[10] When a high-energy photon excites an electron across the band gap, the excess energy is dissipated as heat within the device through thermalization, as depicted by process 1 in Fig. 1b. Process 2 in Fig. 1b represents the semiconductor's transparency to sub-band gap photons within the bandgap region, arising from insufficient transparency of wavelengths below the absorber's bandgap, which are also bandgap-dependent and significant contributors to overall efficiency losses. Another significant loss mechanism involves the recombination of photoexcited electron–hole pairs, shown as process 3 in Fig. 1b. This recombination can be mitigated by ensuring high minority carrier lifetimes in the semiconductor material and has a minimal impact on the theoretical efficiency limit. Additionally, the voltage losses across the contacts and junction are represented by processes 4 and 5 in Fig. 1b losses.

2. Strategies to overcome sub-bandgap photon loss

2.1. Intermediate band solar cells

To date, numerous strategies have been devised to mitigate efficiency losses. Below bandgap losses occur due to the transparency of the device to photons with energies lower than the band gap. It has been proposed that these losses can be addressed by employing two-photon absorption (or multi-photon absorption) or sequential sub-band absorption utilizing an intermediate band (IB).[13] The two-photon approach generally requires light intensities far exceeding normal solar illumination. Alternatively, intermediate band solar cells use an IB to create a system akin to two sub-cells in series (representing valence band (VB)-IB and IB-conduction band (CB) transitions) and one in parallel (VB-CB transition) (Fig. 2a). An ideal IB solar cell needs a total band gap of 1.95 eV to divide into sub-band gaps of 0.71 eV and 1.24 eV, potentially achieving a power conversion efficiency of approximately 63% under high solar concentration (46 050 suns).[13] Although there are concerns about non-radiative recombination and challenges in synthesizing and integrating suitable materials to create an effective intermediate band, extensive research has been conducted using first-generation photovoltaic materials. Techniques such as incorporating QDs with discrete energy levels, adding impurities (*e.g.*, metals with partially filled d orbitals), and doping have all been explored to induce IBs in semiconductors such as III–V, II–VI, silicon, and chalcopyrites.[14] However, these IB solar cells are still in the early stages, with current efficiencies falling short of expectations. Perovskites have also been found as promising candidates for IB solar cells, with examples including Cs_2SnI_6 double perovskite, co-doped $MAPbI_3$, and Mn-doped $CsPbI_2Br$.[15,16] Nevertheless, calculations reveal that perovskite-based IB devices will suffer from significant recombination losses rather than effective electron transitions.[17] To overcome this, IBs need partially filled orbitals - with both empty and full states. Doping with metals like Cr, Mo, In, or Ga in $CsPbX_3$ can create half-filled IBs, potentially raising power

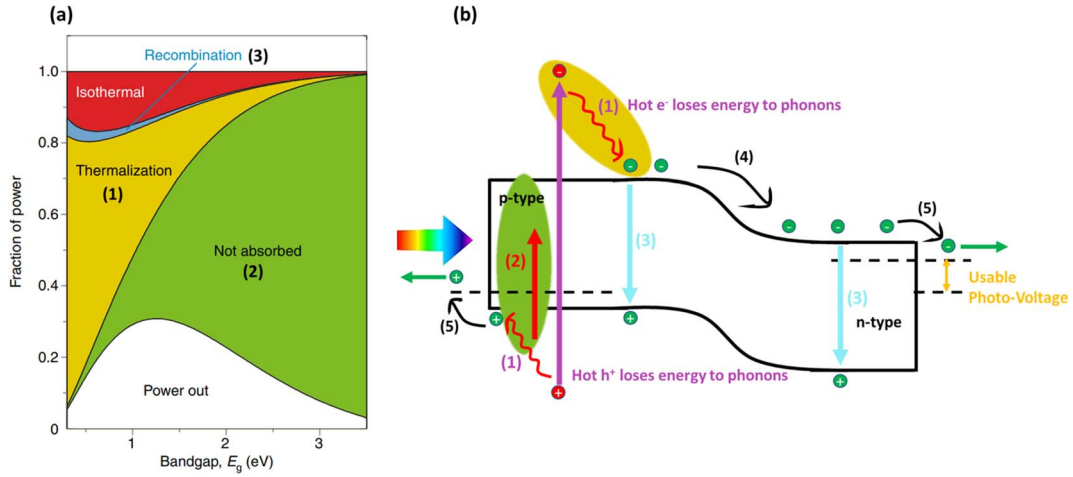

Fig. 1 (a) Intrinsic loss mechanisms in an ideal single-junction PV cell, with respect to E_g. (b) Loss processes in a single junction solar cell: (1) lattice thermalization, (2) below bandgap transparency, (3) recombination, (4) junction loss and (5) contact voltage loss.[10] Adapted from Green, M. A., *Physica E*, 2002,[10] © 2002 Elsevier, with permission from Elsevier *via* Copyright Clearance Center.

conversion efficiencies (PCE) to 55%.[18] Despite promising theoretical calculations, no experimental data has yet confirmed these predictions. Other methods to induce IBs include using QDs in a perovskite matrix, forming periodic cascade energy levels. A recent example using PbS QDs in $MAPbBr_3$ demonstrated IB-assisted photon absorption but achieved low PCE (<1%) due to challenges such as charge transport losses, defects, and interface recombination.[19] While perovskites' chemical flexibility and ease of doping offer significant opportunities for developing IB solar cells, these approaches face substantial hurdles. Key Challenges include non-radiative recombination, optimal doping concentrations, and material integration. Additionally, creating multiple intermediate minibands can constrain light absorption efficiency due to interactions between different states.

Although IBSCs are theoretically capable of exceeding 60% efficiency under concentrated sunlight,[13] their experimental performance has remained well below this threshold. For example, PbS quantum dots embedded in $MAPbBr_3$ matrices have demonstrated intermediate band-assisted absorption but yielded PCEs below 1% due to poor charge transport and severe recombination losses.[21] Efforts to create intermediate bands in perovskites have included the use of transition metal doping, such as Mn-doped $CsPbI_2Br$ and co-doped $MAPbI_3$, aiming to introduce sub-bandgap states that could facilitate sequential photon absorption. However, these approaches often suffer from poor doping control and reduced crystal stability, which hinder the formation of well-isolated, half-filled intermediate bands and instead increase non-radiative recombination losses.[15,22] While theoretical modelling shows potential PCEs approaching 55% with Cr-, Mo-, In-, or Ga-doped $CsPbX_3$,[23] experimental demonstrations are yet to validate these predictions. In addition, practical implementation is complicated by the risk of miniband overlap, sub-band misalignment, and

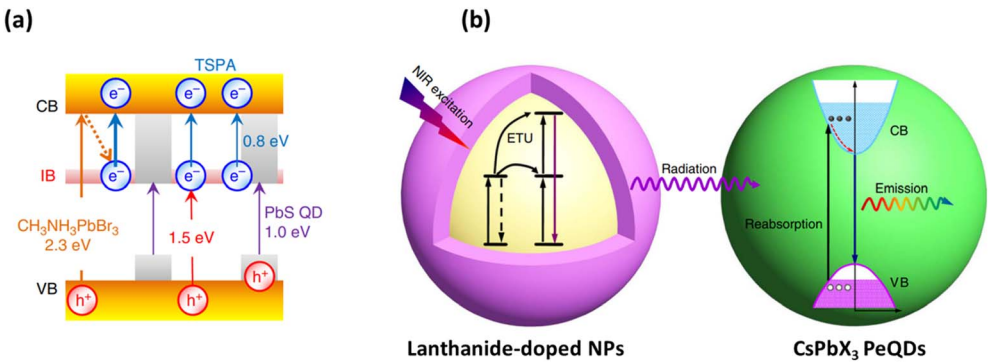

Fig. 2 (a) Schematic energy band diagram of the photo-absorption layer in a IB solar cell. EBG of $MAPbBr_3$ perovskite; 2.3 eV, EBG of PbS QD; 1.0 eV, EVI; 1.5 eV, EIC; 0.8 eV.[19] Reproduced from Hosokawa *et al.*, *Nat. Commun.*, 2019,[19] © The Author(s), under exclusive licence to Springer Nature. Distributed under the terms of the Creative Commons Attribution 4.0 International License (CC BY 4.0) (b) schematic representation of the radiative energy transfer upconversion processes in all-inorganic $CsPbX_3$ perovskite quantum dots through sensitization by lanthanide-doped nanoparticle (the solid and dash lines represent the electronic transitions).[20] Adopted from Zheng *et al.*, *Nat. Commun.*, 2018,[20] © The Author(s), published by Springer Nature, under the terms of the Creative Commons Attribution 4.0 International License (CC BY 4.0).

limited spectral absorption.[24] These hurdles continue to constrain the progress of IBSCs despite significant advances in materials science and device design.

2.2. Upconversion (UC)

Photon upconversion (UC) has been proposed as another innovative optical process that can addresses sub-bandgap photon losses by converting low-energy photons into higher-energy photons, thus significantly advancing photovoltaic technology. UC occurs when two or more photons are sequentially absorbed, followed by the emission of light at a shorter wavelength than the excitation wavelength, a phenomenon known as anti-Stokes emission.[25,26] This process allows light from the infrared spectrum, which typically passes through photovoltaic cells without being absorbed, to be converted into visible light that can be effectively utilized by these devices. A schematic illustration of the radiative energy transfer upconversion process in all-inorganic $CsPbX_3$ perovskite quantum dots facilitated by lanthanide-doped nanoparticles (Fig. 2b).[20] The upconversion process begins with the absorption of NIR excitation light by the lanthanide-doped NPs, followed by successive photon absorption and energy transfer upconversion within the lanthanide ions. This results in the emission of ultraviolet (UV) and visible photons, which are subsequently reabsorbed by the perovskite quantum dots. This energy transfer promotes the generation of electron–hole pairs (excitons) within the conduction band and valence band of the perovskite quantum dots, culminating in photon emission through exciton recombination.

Polycyclic aromatic hydrocarbons (PAHs) are a type of organic molecule that accomplish photon UC through the process of triplet–triplet annihilation (TTA).[25] This involves the interaction of two triplet-state molecules, resulting in the annihilation of one triplet molecule and the formation of a higher-energy singlet molecule, which subsequently emits a photon of higher energy. TTA is highly efficient in specific organic compounds and is an area of active research due to its potential applications in photovoltaic devices and other optoelectronic systems. Inorganic materials, on the other hand, exhibit UC through different mechanisms, primarily involving ions of d-block or f-block elements such as lanthanides (Ln^{3+}), titanium (Ti^{2+}), nickel (Ni^{2+}), molybdenum (Mo^{3+}), rhenium (Re^{4+}), and osmium (Os^{4+}). These ions can participate in three fundamental UC mechanisms: energy transfer upconversion (ETU), excited-state absorption (ESA), and photon avalanche (PA).[27] ETU occurs when an ion in an excited state transfers its energy to a neighbouring ion, which is already in an excited state. This transfer promotes the second ion to an even higher energy level, from which it can emit a higher-energy photon. ETU is particularly efficient in materials doped with lanthanide ions, such as Er^{3+} or Yb^{3+}, which have long-lived excited states that facilitate energy transfer. In contrast, ESA involves the sequential absorption of two or more photons by a single ion. The ion first absorbs a photon and is excited to a higher energy level. While in its excited state, it absorbs another photon, which elevates it to an even higher energy level, after which it can emit a photon of higher energy. ESA is commonly observed in transition metal ions like Ti^{2+} and Ni^{2+}. Finally, PA is a less common but highly efficient UC mechanism where the absorption of a photon leads to a chain reaction of energy transfers and absorptions, resulting in the emission of multiple higher-energy photons. This process requires a precise balance of energy levels and interactions between ions, making it challenging to achieve but highly effective when realized. Thermal upconversion has also been introduced as another promising approach, where low-energy photons are absorbed by the up-converter material and converted to heat.[28,29] This heat can then be used to emit higher-energy photons. By carefully designing the up-converter's density of optical states, as well as frequency- and angular-selective emission characteristics, a more efficient UC process can be achieved. Photonic crystal designs enable the realization of these surface features, and their use in thermophotovoltaics and passive radiative cooling has been demonstrated both theoretically and experimentally. A planar thermal up-converting platform can have a front surface that efficiently collects low-energy photons incident within a specific angular range and a back surface that efficiently emits only high-energy photons.

UC materials can be incorporated into photovoltaic devices in various forms, including bulk crystals, optical fibres, and nanoparticles. Each form has its advantages and challenges. Bulk crystals and optical fibres can provide high UC efficiency but may be difficult to integrate into thin-film solar cells. Nanoparticles, on the other hand, offer flexibility in integration but may suffer from lower UC efficiency due to surface quenching effects and other size-related phenomena.[30] In recent years, there have been some notable achievements in incorporating UC materials into solar cells. For example, research has demonstrated the potential for UC nanoparticles to enhance the efficiency of dye-sensitized solar cells and organic photovoltaic cells.[31,32] Studies have reported efficiency improvements of several percentage points. Yet, despite the significant potential of UC for enhancing photovoltaic technology, several bottlenecks remain. One major challenge is the efficiency of the UC process itself. While some materials exhibit high UC efficiency in laboratory conditions, maintaining this efficiency in real-world operational conditions is difficult. Factors such as non-radiative decay, concentration quenching, and the stability of UC materials under continuous illumination and varying environmental conditions can significantly reduce performance. Another critical issue is the integration of UC materials into existing photovoltaic systems. This involves not only the physical incorporation of UC materials into solar cells but also ensuring that the upconverted photons can be efficiently absorbed by the photovoltaic material. For instance, the emission spectrum of the UC material must overlap well with the absorption spectrum of the photovoltaic material to ensure efficient energy transfer. Cost and scalability are also significant challenges. Many of the materials that exhibit high UC efficiency, such as certain lanthanide-doped compounds, are expensive and difficult to synthesize in large quantities. As such, developing cost-effective and scalable methods for producing UC materials is essential for their widespread adoption in

photovoltaic applications. While upconversion addresses the inefficiency of sub-bandgap photon loss by converting low-energy photons to usable ones, the complementary strategy of downconversion tackles the thermalisation loss of high-energy photons. This will be further discussed in Section 3.5 as part of thermal loss mitigation.

UC addresses the inefficiency of sub-bandgap photon loss by converting low-energy photons into usable ones through nonlinear optical processes, typically involving rare-earth ions such as Er^{3+} and Yb^{3+}. While this conceptually extends the spectral response of photovoltaic devices, its practical implementation remains limited. UC layers have demonstrated external quantum efficiency (EQE) enhancements of 2–4% under concentrated near-infrared illumination in silicon solar cells; however, under standard one-sun conditions, the enhancement is minimal due to the low absorption cross-sections of rare-earth ions and the requirement for high photon flux to activate efficient UC processes.[33] Additionally, challenges such as spectral mismatch between UC emission and the absorption band of the active layer, as well as thermal quenching at operational temperatures, significantly constrain UC effectiveness.[34,35] To mitigate these issues, current research focuses on developing materials with broadened absorption bands and higher quantum yields at lower excitation intensities, and on embedding UC phosphors within plasmonic or photonic architectures to enhance local field effects and light–matter interaction strength.[36]

3. Strategies to mitigate hot carrier thermalization loss

In single-junction solar cells, two major intrinsic energy losses depend on the bandgap energy (E_g) of the absorbing layer, as shown in (Fig. 1a and b). Thermalization and below bandgap losses are the primary loss mechanisms, together accounting for over 50% of the total energy loss across an E_g range of 0.5 to 3.0 eV. Thermalization loss happens when photocarriers are generated by photons with an energy much higher than the bandgap, leading to a rapid cooling (thermalization) process to the band edges (Fig. 1b). These high-energy charge carriers, known as "hot carriers", have excess kinetic energy above the conduction or below the valence bands, resulting in initial temperatures above the "lattice temperature -the equilibrium temperature of the crystal lattice in the absence of external excitation." In typical semiconductors, hot carriers have short lifetimes, such as 2 ps in GaAs and 10 ps in InN films.[37,38] However, in halide perovskites, strong electron-phonon coupling (Fröhlich interaction), the polaronic nature of the carriers, the phonon bottleneck effect, and other proposed mechanisms result in significantly longer lifetimes for hot carriers, such as 1000 ps in $FASnI_3$ films and over 2500 ps in $MAPbI_3$ films.[39,40] Additionally, lower-dimensional perovskites with quantum and dielectric confinement exhibit even slower cooling of hot carriers.[41] To surpass the SQ limit and achieve an ultra-high PCE, effectively utilizing hot carriers is essential. Two main approaches have been proposed to supress the thermalization losses: (i) extracting hot carriers before they cool to the band edge, which could potentially produce an open-circuit voltage (V_{OC}) greater than the bandgap energy - the basic principle of hot-carrier solar cells. This requires an ultrafast extraction process, on the order of sub-picoseconds, between the absorbing layer and charge transfer layers. (ii) Enhancing the photocurrent by multiplying the electron–hole pairs through impact ionization, known as multiple exciton generation (MEG). This approach aims to achieve an internal quantum efficiency (IQE) greater than 100%, *i.e.*, IQE > 1, indicating that more than one charge carrier pair is generated per absorbed photon.

3.1. Hot carrier solar cells (HCSCs)

As discussed above, in conventional solar cells, electron–hole pairs generated by photon absorption lose excess energy as they cool from their initial high-energy ("hot") state to the band edges, primarily through optical phonon emission. Hot carrier solar cells (HCSCs) aim to minimize energy loss by extracting carriers while they remain at elevated energy levels within a narrow energy range. This process relies on two critical components: a significant reduction in carrier cooling within the hot carrier absorber (HCA) and selective carrier extraction through energy-selective contacts (ESCs).[42] Fig. 3a illustrates the carrier transport mechanism, where hot carriers are extracted through ESCs within a defined energy range, while the output voltage is determined by the chemical potential difference between the extracted carriers, reduced by any energy loss from carrier cooling during extraction.[43] Efficient extraction further depends on quasi-ballistic carrier transport, allowing elastic carrier–carrier scattering to minimize extraction time. Fig. 3b highlights the general structure of an HCSC, consisting of a light absorber layer sandwiched between two ESCs.[44] These contacts establish narrow energy windows that selectively permit the extraction of high-energy carriers while blocking cooled carriers, ensuring effective charge separation and collection.

The operational principle of hot carrier solar cells revolves around maintaining the energetic distribution of photo-generated carriers long enough to enable efficient extraction before thermalization occurs. To achieve a photovoltage exceeding the bandgap energy (E_g), the transport time of hot carriers within the semiconductor lattice and their extraction at the absorber layer/electron transfer layer (ETL) or hole transfer layer (HTL) interfaces must be shorter than their cooling time. This process must be complemented by rapid collection at the electrodes to minimize recombination losses.[45] Hot carriers initially follow a Boltzmann distribution within the density of states (DOS) before relaxing to the conduction band minimum (CBM) and valence band maximum (VBM). By delaying this relaxation and ensuring swift extraction, hot carrier solar cells can surpass the efficiency limits of conventional photovoltaic devices. Boosting the open-circuit voltage in hot-carrier solar cells involves using resonant tunnelling states, known as "energy selective contacts."[46] This method requires materials with an ideal bandgap, long carrier relaxation times, high

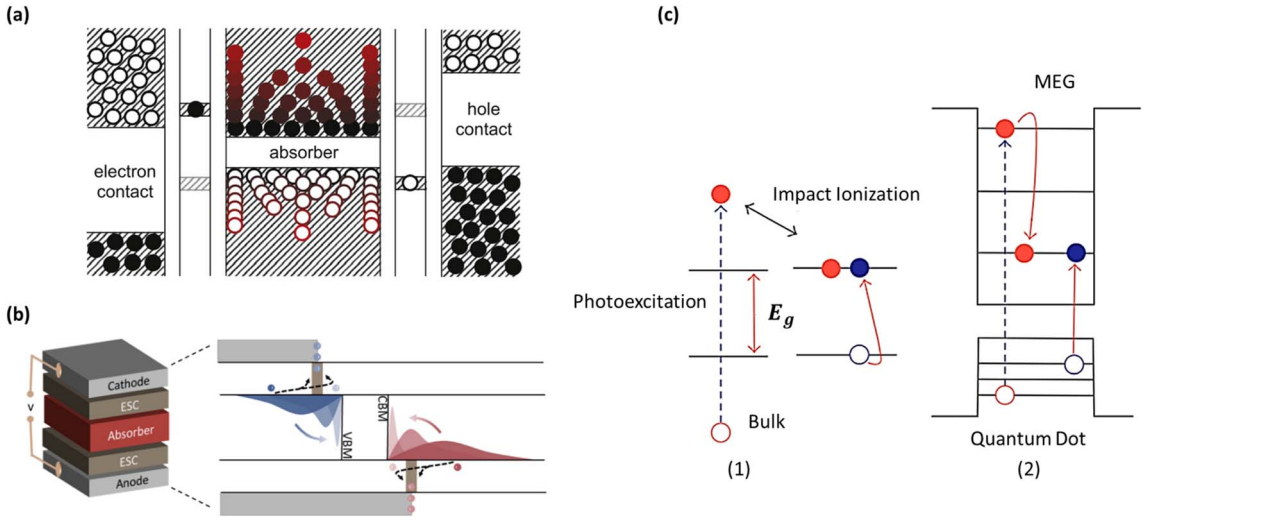

Fig. 3 (a) Schematic of hot carrier transport in an HCSC, illustrating carrier extraction through energy-selective contacts (ESCs) and the corresponding output voltage.[43] Reproduced from D. König *et al.*, *Physica E*, 2010,[43] with permission from Elsevier (b) Schematic of an HCSC device structure with ESCs and the associated energy diagram, highlighting the conduction band minimum (CBM) and valence band maximum (VBM).[44] Reproduced from Lin *et al.*, *ACS Energy Lett.*, 2024,[44] under the terms of the Creative Commons Attribution 4.0 International License (CC BY 4.0). (c) Generation of multiple excitons from highly excited electron–hole pairs. (1) In a bulk semiconductor, the excited electron relaxes to the bandgap. (2) In QDs, impact ionization, the inverse of the Auger process, occurs at a much higher rate than in bulk materials, a phenomenon often referred to as multiple exciton generation (MEG) in QDs.[51] Adapted from Serafini *et al.*, *Journal of Nanotechnology*, 2018, under the terms of the Creative Commons Attribution 4.0 International License (CC BY 4.0).

absorption efficiency, a wide photonic bandgap, and excellent carrier mobility. These characteristics allow the selective transmission of hot carriers while blocking lower energy carriers, thus optimizing the output voltage. The goal is to capture the excess energy of hot carriers before it dissipates as heat, thereby enhancing device efficiency beyond traditional limits. Achieving a V_{oc} that exceeds the semiconductor bandgap demands suitable materials and innovative engineering solutions.

Graphene is promising for HC solar cells due to its properties as a gapless semimetal with linear band dispersion near the Dirac point.[47,48] High-energy photocarriers relax to lower energies near this point, stalling carrier relaxation, a phenomenon known as the phonon bottleneck effect. This increases the probability for carriers to tunnel through the contact electrode, potentially boosting the open-circuit voltage. However, graphene's low optical absorption (approximately 2.3% per layer for visible light) limits its solar energy conversion efficiency. Researchers are integrating heterostacked van der Waals layers between graphene and semiconductor absorbers like MoS_2, $MoSe_2$, WSe_2, and $MoTe_2$.[49,50] This setup aims to enhance absorption while minimizing interface defects and traps, crucial for maintaining high carrier mobility and reducing recombination losses. The graphene/MoS_2 heterostructure demonstrates this approach, achieving high hot electron temperatures (around 2000 K), prolonged relaxation times (picoseconds), and reduced carrier–phonon interactions. Despite these advances, significantly enhancing the open-circuit voltage in hot-carrier solar cells remains challenging. Optimal materials for "smart" contact electrodes must have high conductivity, transparency, and accommodate a range of tunnelling energy states to maximize HC solar cell efficiency.

To achieve hot carrier solar cells, several key factors must be addressed in future research efforts: (i) Reducing the rate of hot carrier cooling in the light absorber. (ii) Ensuring proper energy level alignment, where the energy levels of the electron transfer layer (ETL) and hole transfer layer (HTL) are matched to the energy distribution of hot carriers in the active layer, which follows the Boltzmann distribution. This alignment should also account for the density of states (DOS) of the active layer material, which is determined by atomic orbital (AO) interactions and defines the available energy states for carriers. (iii) Enabling ultrafast extraction of hot carriers at the active layer and contact interfaces to minimize energy loss during transport. (iv) efficient external transport (collection) of carriers at the electrodes to minimize recombination losses. Unless all these requirements are met simultaneously, the ambition of a device possessing a longer cooling time than its combined transport and extraction times is not realistic. Nonetheless, several recent experimental efforts have demonstrated encouraging progress toward realising hot carrier solar cells. For example, van der Waals heterostructures such as graphene/MoS_2 have shown hot electron temperatures exceeding 2000 K and picosecond-scale relaxation times, benefiting from phonon bottleneck effects and reduced carrier–phonon interactions.[49,50] These systems also exhibit energy-selective carrier extraction and are being explored as platforms for prototype HCSC architectures. Furthermore, Lin *et al.* recently proposed a functional HCSC device structure incorporating energy-selective contacts, highlighting its potential to generate photovoltages beyond the bandgap through resonant tunnelling extraction.[44] While fully

operational devices remain a significant challenge, these advancements demonstrate that key elements of the HCSC concept are becoming increasingly feasible.

Despite significant theoretical potential and rapid material advances, the practical performance of hot carrier solar cells remains far below commercial standards. Demonstrated devices based on nanostructured InAs/GaAs quantum wells or graphene-semiconductor heterostructures have exhibited photovoltages approaching or slightly exceeding the absorber bandgap, but PCEs are typically below 2–3%.[48,52,53] The main limitations stem from rapid hot carrier cooling (typically within 1–5 ps in bulk materials), poor selectivity of energy-filtering contacts, and losses at imperfect interfaces.[53] Moreover, fabricating energy-selective contacts that combine sharp energy cutoffs with high transparency and conductivity remains technologically challenging. Device-level implementation also requires integration of ultrafast carrier extraction layers with low defect densities, which has so far proven difficult outside of lab-scale proof-of-concept systems.[54] While recent heterostructures based on 2D materials show promise, scalable architectures and reliable performance benchmarks are still under development.

3.2. Multiple exciton generation

Splitting a single hot electron–hole pair into multiple pairs can be achieved through multiple exciton generation (MEG), as depicted in (Fig. 3c). MEG requires the impact ionization rate to surpass the cooling rate, allowing multiple excitons to form and can result in an EQE exceeding 100% at certain wavelengths.[55,56] Traditional (photovoltaic) semiconductors typically have rapid carrier relaxation times and strong charge screening (weak carrier–carrier interactions). These limitations weaken carrier–carrier scattering and reduce exciton binding energy, resulting in high threshold energies, typically over three to four times the bandgap, which culminates in relatively modest MEG efficiencies, such as the approximately 40% observed in PbS films.[57] The pursuit of materials that optimize MEG has driven researchers to explore alternatives beyond traditional bulk semiconductors. By quantizing energy levels and spatially confining hot carriers, momentum conservation can relax, enhancing many-body interactions among carriers. Consequently, higher MEG yields are expected to be observed in QD systems compared to their bulk counterparts.[58,59] Several research groups have observed MEG in QD nanocrystals, indicating potential for MEG solar cells.[59,60] QDs, including PbSe, CdSe, $CuInSe_2$, and Si, present a compelling alternative due to their quantum confinement effects.[61,62] Due the strong spatial overlap of the excited state wavefunctions these materials exhibit enhanced Coulomb interactions, significantly improving MEG efficiency by achieving threshold energies near three times the bandgap, with efficiencies reaching up to 70%. However, device-level demonstrations are still lacking. In practical devices, slower hot carrier cooling is crucial to provide sufficient time for MEG to occur. This is essential for achieving a photovoltage greater than the bandgap energy (E_g), as seen in ultrafast hot carrier extraction achieving $V_{OC} > E_g$.[63] In traditional IV–VI QD MEG solar cells, enhancing MEG has been achieved through optimizing QD ligand chemistry, constructing core–shell (heterostructure) architectures, and selecting suitable QD materials.[64,65] Despite these advancements, poor charge transport and extraction remain significant challenges, primarily due to under-coordinated surface atoms that create surface states capable of trapping a substantial portion of photocarriers and reducing the V_{OC}. An alternative quantum form, quasi-2D multiple quantum well (MQW) perovskites, show promise.[66] However, research on the MEG effect in quasi-2D MQW/superlattice perovskites is still in its infancy. From a device perspective, quasi-2D perovskites should be positioned between asymmetric electrodes with an edge-on stacking configuration to ensure efficient charge transport perpendicular to the electrode plane. Van der Waals-layered materials, such as $MoTe_2$ and WSe_2 films, have shown significant promise in MEG. These materials exhibit an ideal threshold energy near twice the bandgap and CM efficiencies up to 99%, as confirmed by transient absorption spectroscopy and direct photocurrent measurements.[67] This advancement suggests a notable increase in short-circuit current with higher photoexcited energy. Although improved conductivity is an advantage of these two-dimensional films, high Schottky barrier resistance between the channel and metal electrode still limits overall solar cell performance. Nevertheless, van der Waals-layered semiconductors pave the way for a new era of CM solar cells with markedly enhanced efficiency.

Despite numerous demonstrations of MEG in quantum dots and 2D materials, translating these phenomena into practical photovoltaic gains remains a key challenge. Device-level EQEs exceeding 100% have been observed under high-energy photon excitation, particularly in PbSe and VO_2 systems, but these results often rely on non-standard measurement conditions or ultrafast laser setups.[54,68,69] The main bottlenecks include inefficient exciton extraction, Auger recombination, and carrier trapping at QD interfaces. Perovskite quantum dots have shown promise due to tunable bandgaps and improved defect tolerance, but surface passivation and charge transport remain critical barriers to achieving high open-circuit voltages in MEG-enabled devices.[70] Recent hybrid systems combining PQDs with conjugated polymers have demonstrated improved environmental stability and photoresponse, offering a promising path toward scalable MEG architectures.[71] Nonetheless, widespread implementation will depend on further advances in interface engineering and low-threshold MEG material design.

3.3. Singlet fission

Singlet fission (SF) in mixed perovskite and organic chromophore systems is a promising approach for achieving multiple exciton generation (MEG) in solar cells. SF occurs in organic chromophores like pentacene and rubrene, where one excited singlet state transforms into two triplet states, with quantum yields exceeding 200%. Recent advancements in SF-enhanced solar cells have shown total exciton yields up to 133%, external quantum efficiencies (EQE) up to 130%, and internal quantum efficiencies (IQE) up to 170%.[72,73] Maintaining high

quantum yields under real-world conditions, integrating SF materials into stable devices, and optimizing performance across varying environments are the main barriers to efficient practical applications. Key challenges include finding efficient exciton fission materials, ensuring effective charge carrier separation, and achieving long-term stability. Finding the practical strategies to enhance MEG quantum yield, designing optimal bandgaps to maximize light absorption (while minimizing optical losses), and developing innovative device structures to mitigate Shockley-Read-Hall recombination losses are critical to advance this strategy.

Recent advancements have demonstrated the potential of singlet fission (SF) to enhance solar cell performance, with external EQEs exceeding 100% in specific tandem configurations. For instance, a silicon–singlet fission tandem solar cell achieved an EQE surpassing 100% at the absorption peak of pentacene, confirming efficient photocurrent addition and high spectral stability under sunlight.[74] Moreover, the integration of SF materials with perovskite layers has shown improved ultraviolet stability and enhanced device efficiency, offering hybrid strategies for both performance and durability.[75] Other work using tetracene oligomers has enabled intramolecular singlet fission and efficient triplet exciton harvesting, further advancing the material design of SF-based photovoltaics.[76] Despite these developments, practical deployment is hindered by challenges such as suboptimal energy level alignment, inefficient triplet extraction, and limited long-term operational stability under real-world conditions.[77] Continued research on interface engineering, triplet transfer dynamics, and material stability is essential for unlocking the full potential of SF-enhanced solar cells.

3.4. Tandem solar cells

Another approach to improving the PCE of solar cells involves using multiple junctions with progressively narrower band gaps, reducing carrier relaxation losses and boosting device voltage. Tandem or multijunction cells significantly enhance PCE by stacking layers of materials with varying bandgaps, allowing them to utilize around 86% of the solar spectrum.[78] Tandem solar cells are typically classified into two configurations: four-terminal (4T) and two-terminal (2T) designs. In 4T TSCs, the subcells are optically coupled but electrically independent, allowing each subcell to be fabricated and optimized separately without constraints related to fabrication methods, temperatures, or cell polarities (Fig. 4a–c).[79] This independence enables higher individual efficiencies but comes with increased optical losses due to parasitic absorption and reflections from transparent conductive oxide layers. Additionally, the complexity of fabrication, assembly, and the need for multiple substrates contribute to higher overall costs, limiting their industrial application. In contrast, 2T TSCs feature both optical and electrical coupling between subcells (Fig. 4d–f).[79] This design simplifies system integration, reduces material usage, and lowers installation costs. However, achieving efficient 2T TSCs remains challenging due to the need for precise current and lattice matching, processing compatibility between subcells, and the incorporation of effective recombination layers (RLs) or tunneling junctions (TJs).[80] Without a properly designed TJ or RL, the formation of an opposing p–n junction between subcells can reduce the open-circuit voltage (V_{oc}) and overall performance.

Polymers are extensively used in third-generation solar cells, including DSSC, PSC, and tandem solar cells, to improve efficiency.[81] Seminal work by You *et al.* reported a low-bandgap polymer with high mobility and a bandgap of 1.38 eV, achieving a 10.6% efficient solution-processed tandem solar cells.[82] Despite their advantages, organic photovoltaic cells often exhibit lower performance due to the limited charge mobility of organic materials, which restricts active layer thickness and light absorption. Meng *et al.* employed a semi-empirical model and a tandem cell strategy to achieve a 17.29% efficient two-terminal monolithic solution-processed tandem organic solar cell, leveraging the tunable bandgap and high diversity of OPVs.[83]

Perovskite solar cells, with adjustable bandgaps ranging from 1.48 to 2.23 eV and high absorption, are particularly suitable for tandem configurations.[84] Innovative techniques like "boosted solvent extraction" have improved perovskite film thickness while maintaining smoothness, resulting in PCEs of 34.6% for stacked perovskite cells above silicon.[85] Mechanically stacked two-terminal perovskite/Si tandem solar cells have achieved efficiencies up to 26.3% by optimizing sub-cells separately and connecting them to reduce optical losses.[86] Wide-bandgap MHPs showed early potential for achieving PCEs above 30%, though challenges like photoinduced low open-circuit voltages and phase segregation persist.[87] Recent advancements have demonstrated PCEs exceeding 30% for perovskite/silicon tandem cells.[88] Despite these advancements, significant challenges remain for the broad development and commercialization of tandem solar cells.

The stability and degradation of perovskite materials, which are central to many tandem solar cell designs, continue to pose major challenges. These materials are sensitive to environmental stressors such as moisture, oxygen, heat, and UV exposure, all of which can accelerate degradation through pathways like ion migration, interface decomposition, and phase segregation.[89,90] To mitigate these effects, various strategies have been explored, including advanced encapsulation techniques, interface passivation, compositional engineering (*e.g.*, triple-cation and mixed-halide formulations), and the development of wide-bandgap perovskites less prone to halide segregation.[91,92] Despite progress, the long-term operational stability of perovskite-based tandem devices under real-world conditions remains a critical and unresolved issue. Another layer of complexity arises in the integration of the perovskite top cell with the silicon bottom cell, where thermal expansion mismatch, interfacial incompatibility, and spectral mismatch can reduce both efficiency and reliability.[93–95] Innovations such as inverted (p-i-n) architectures, interlayers, and recombination junctions have improved performance but have yet to fully solve the durability challenge at scale. In parallel, manufacturing issues such as large-area uniformity, defect tolerance, and reproducibility have limited commercial readiness. Scalable

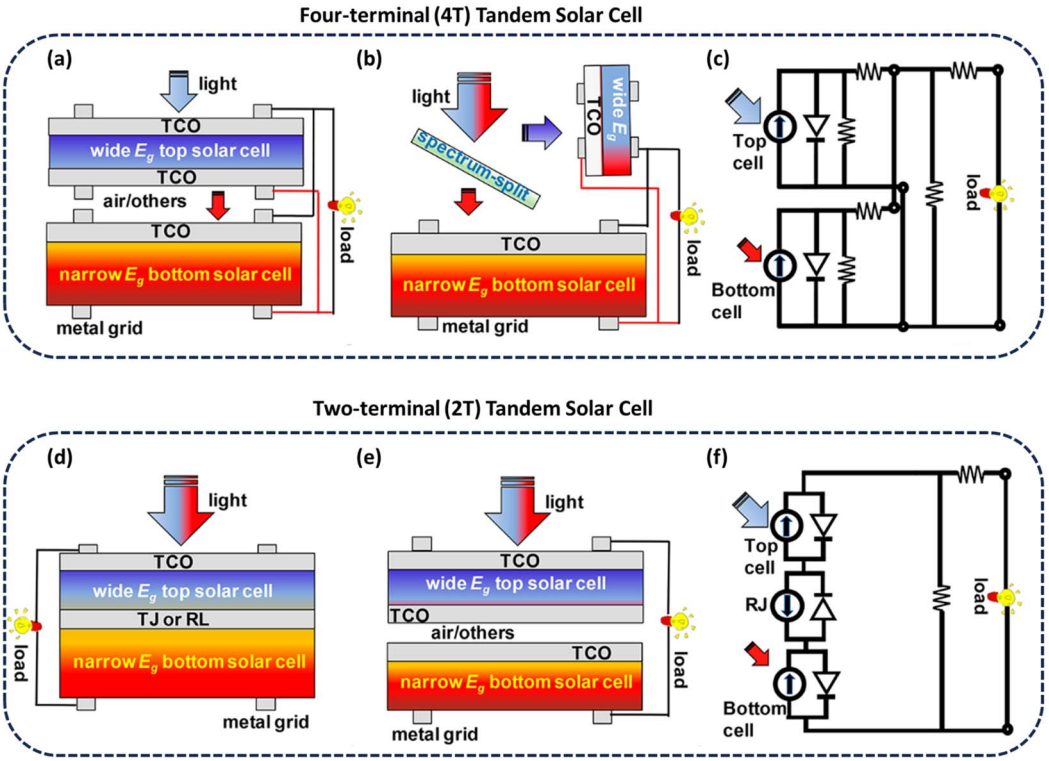

Fig. 4 Schematic diagrams of 4T TSCs (a) without and (b) with a spectrum split. (c) Equivalent circuit of a 4T TSC. (d and e) Schematic diagrams of 2T TSCs. (f) Equivalent circuit of a 2T TSC.[79] Adopted from H. Li and W. Zhang, *Chem. Rev.*, 2020,[79] with permission from the American Chemical Society.

processes like slot-die coating and blade coating have shown promise in pilot settings, but require further optimisation for industrial production.[96,97] Over the past decade, perovskite solar cells have indeed been hailed as a potential "revolution" in photovoltaics, particularly for tandem applications, but the gap between laboratory performance and commercial durability remains significant. While remarkable progress has been made in achieving PCEs over 30%, stability under prolonged stress and large-scale processing remain key bottlenecks. Current research is increasingly focused on developing compositionally robust materials, interface-stable device designs, and manufacturing protocols that are tolerant to ambient variations. A critical consensus in the field now recognises that solving these practical challenges is essential for fulfilling the early promises of perovskite tandem solar cells.

3.5. Down-conversion

In addition to the upconversion strategies described earlier, which focus on recovering low-energy photons, downconversion (DC) and downshifting (DS) represent alternative approaches that target high-energy photon losses. While UC often requires multi-photon or nonlinear processes with stringent material conditions, DC is considered more practically achievable in some cases due to simpler mechanisms like quantum cutting, particularly with rare-earth-doped systems. Down-conversion (DC) and downshifting (DS) are advanced techniques that hold promise for enhancing solar cell efficiency by addressing specific photon loss mechanisms. DC targets thermalization losses, where high-energy photons are typically lost as heat in traditional solar cells, by converting them into multiple lower-energy photons that can be more effectively utilized by the solar cell's active layer.[98] DS, on the other hand, focuses on reducing surface recombination losses by shifting the energy of absorbed photons to better match the bandgap of the solar cell material, thereby improving the conversion efficiency.[56] Traditional solar cells primarily absorb light in the visible spectrum, where a significant portion of the sun's energy is concentrated. However, they often fail to efficiently utilize photons from the ultraviolet (UV) or infrared (IR) regions. DC involves converting high-energy UV photons into multiple lower-energy visible or near-infrared photons, potentially achieving quantum efficiencies greater than unity (Fig. 5a). This process relies on host lattice states or rare-earth ions, which split a single high-energy photon into two or more lower-energy photons, enhancing absorption in the cell's active layer. In contrast, DS focuses on converting a high-energy photon into a single lower-energy photon with a longer wavelength, improving spectral matching between incident light and the solar cell's absorption characteristics. This process begins when a high-energy photon excites the material from the ground state $G(S_0)$ to an excited state, such as $E_1(S_1)$ or $E_2(S_2)$. The excited state can relax non-radiatively through internal conversion before emitting a lower-energy photon *via* Stokes luminescence (Fig. 5b). While DS does not achieve quantum efficiencies greater than unity, it

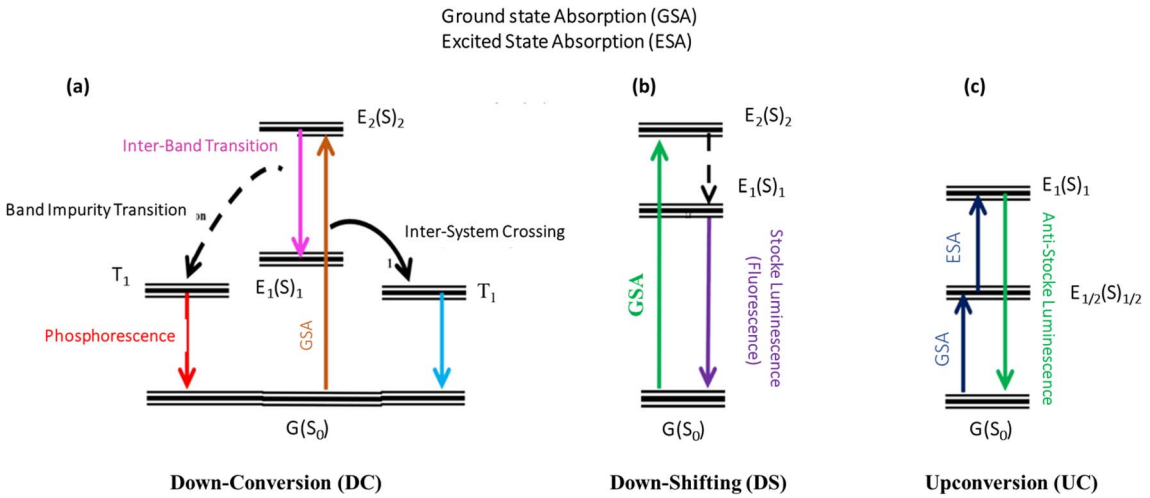

Fig. 5 Schematic representation of phenomenon's of (a) downconversion (DS), (b) down shifting (DS), and (c) upconversion (UC).[34] Adopted from Nowsherwan *et al.*, *J. Mater. Sci.*, 2024,[34] with permission from Springer Nature. © 2024, The Author(s), under exclusive licence to Springer Nature.

still enhances performance by reducing surface recombination losses and ensuring more efficient photon absorption. Furthermore, while DC enhances photon yield by generating multiple lower-energy photons, DS focuses solely on optimizing spectral compatibility without increasing the total photon count. Both mechanisms complement upconversion (Fig. 5c), which works oppositely by converting multiple low-energy photons into a single higher-energy photon.

Recent studies by research groups have shown specific improvements in solar cell performance through the integration of down-conversion (DC) and down-shifting (DS) materials with a reported increase in EQE from 70% to over 90% in the UV and near-infrared regions.[99,100] This enhancement was achieved by doping silicon solar cells with rare-earth ions, effectively converting high-energy UV photons into lower-energy photons that better match the silicon bandgap. This strategy led to a significant increase in the short-circuit current density (J_{sc}), with reported values exceeding 40 mA cm^{-2} compared to standard values around 35 mA cm^{-2}.[99,100] Consequently, these improvements contributed to raising the PCE of the solar cells from approximately 20% to over 25%, showcasing the efficacy of DC and DS technologies to enhance solar energy harvesting capabilities. However, several challenges hinder their widespread implementation in commercial photovoltaic technologies. One significant challenge is the stability and efficiency of materials under prolonged exposure to solar radiation. Many rare-earth-doped materials exhibit high conversion efficiencies in controlled laboratory conditions but degrade over time when exposed to sunlight, limiting their practical longevity and reliability in outdoor environments.[101] Achieving stable performance over extended periods remains a critical research focus.

Integration with existing solar cell technologies presents another hurdle. The DC or DS layer must complement the solar cell's materials without introducing additional losses or compromising overall device performance. Achieving seamless integration requires precise control over the emission properties of DC and DS materials, which can be difficult to achieve consistently in practical applications. Furthermore, the cost and scalability of DC and DS technologies pose significant barriers to their widespread adoption. The production of high-efficiency materials, particularly those incorporating rare-earth elements are costly and challenging to scale up. Cost-effective manufacturing processes and scalable production methods are still needed to make DC and DS technologies economically viable for commercial deployment. In contrast to UC, which remains limited by low efficiency under standard solar illumination, DC and DS approaches benefit from more favourable photon conversion pathways and simpler integration requirements, though they too face challenges in material stability and cost.

Despite promising results in enhancing device performance through downconversion and downshifting strategies, the lack of standardised testing protocols continues to hinder meaningful comparison across studies.[102] Reported improvements often vary widely due to differences in experimental setups, spectral converter placement, solar cell architecture, and the absence of encapsulation layers or long-term stability testing.[102] In many cases, prototype solar cells are miniaturised, lack realistic module configurations, or are evaluated under laboratory conditions that do not reflect field operation.[103,104] Moreover, the spectral mismatch between solar simulators and the narrow emission/absorption bands of some spectral converters introduces additional uncertainty, particularly when simulators are optimised for broadband silicon cells.[105] These issues collectively highlight the need for more rigorous benchmarking standards to evaluate the true impact of spectral conversion materials in real-world photovoltaic environments.[102,105] Recent work by Belançon *et al.* has drawn attention to these limitations, especially the challenges of integrating glass-based luminescent materials in silicon-based modules and the importance of standardising spectral simulator outputs for narrowband devices.[106] As spectral modification

technologies move closer to application, addressing these benchmarking challenges will be essential for assessing true performance gains and guiding material development. To unlock the practical potential of DC and DS technologies, future efforts must focus on ensuring long-term operational stability, seamless integration with commercial photovoltaic architectures, and the development of standardised evaluation protocols that reflect real-world performance conditions.

4. Simultaneous mitigation of sub-bandgap and thermalization losses

Recent advances in the understanding of MHPs have revealed intriguing possibilities for managing intrinsic energy losses that fundamentally limit single-junction solar cell performance. A key emerging concept is the lattice energy reservoir (LER): a dynamic, long-lived nanodomain within the soft perovskite lattice that stores phonon energy transferred from hot photocarriers through strong electron–phonon and phonon–lattice coupling.[107–113] Although direct experimental verification of the LER is still pending, a number of unique and reproducible behaviours observed in MHPs provide compelling indirect evidence for its existence, including anomalous phenomena such as an exceptionally longer[114] carrier recombination lifetime than that predicted by Langevin theory,[115,116] slowed cooling of hot carriers,[117] defect tolerance,[118–120] anomalous upconversion fluorescence (exclusive multi-photon absorption and lanthanum-doping),[121,122] as well as persistent structural polarization,[123] memory,[124,125] and ultraslow variations in photoluminescence (PL) efficiency and carrier lifetime (also referred as to defect healing, defect curing, photobrightening).[126–129] These phenomena, especially the unusually long carrier and lattice relaxation times (ranging from milliseconds to even seconds), point to the existence of an internal mechanism capable of energy retention and gradual release. This stands in sharp contrast to the ultrafast cooling dynamics typically observed in conventional semiconductors.[123,130–132]

LERs are proposed to form within localized nanodomains of the MHP lattice, where strong carrier-lattice coupling creates an energetically elevated and metastable state that can act as a temporary energy retention medium. Rather than dissipating immediately as heat, this retained vibrational energy remains dynamically coupled to the electronic system and can participate in secondary processes such as delayed carrier excitation or phonon-assisted upconversion.[91–93] The formation of LERs is enabled by the soft and anharmonic nature of the MHP lattice, in conjunction with phonon bottleneck effects, strain-induced phonon reflection, and limited acoustic phonon transport, factors that collectively confine vibrational energy in specific regions.[123,133] Fig. 6a, schematically illustrates how LERs could serve as multifunctional energy reservoirs: hot phonon energy, typically lost *via* lattice thermalisation (Loss 1), is retained and later used to drive the upconversion of carriers originating from NIR sub-bandgap photon absorption (Loss 2). In this scheme, NIR-excited carriers in a MHP-NIR composite are first transferred into metastable sub-bandgap states and then promoted to the conduction band *via* phonon-assisted transitions, enabling simultaneous recovery of thermal and sub-bandgap energy losses within a unified process.

This dual-interaction framework represents a novel mechanism for energy recycling in single-junction solar absorbers. Unlike conventional strategies that tackle either hot carrier losses or sub-bandgap transmission in isolation, the LER paradigm integrates both within a single carrier-lattice coupling process. Notably, the phonon-driven upconversion mechanism in this model is based on single-photon events and linear energy transfer pathways, rather than relying on multi-photon or nonlinear optical processes. This distinction offers a conceptual pathway to enhanced efficiencies under standard solar conditions.[107] Fig. 6b illustrates the conceptual operation of a lattice-battery solar cell (LBSC), an emerging photovoltaic design that directly leverages the proposed LER within the perovskite absorber to achieve dual-mode energy harvesting. Unlike conventional solar cells that dissipate hot phonon energy as heat, LBSCs aim to store this energy temporarily in the lattice and later reuse it to promote sub-bandgap carriers to the conduction band, thus mitigating both thermalisation and transmission losses in a single-junction device. Structurally, the LBSC adopts a layered architecture similar to standard perovskite devices, comprising an electron transport layer (ETL), a perovskite-NIR composite active layer, and a hole transport layer (HTL), but with distinct photophysical pathways.[107] Output 1 arises from above-bandgap photon absorption, as in typical perovskite solar cells, while Output 2 represents carriers excited from NIR-photogenerated and transfer into the metastable states of perovskite *via* phonon energy released from the LER. This second channel is a key innovation: it enables single-photon upconversion without relying on nonlinear optics or rare-earth doping, instead using intrinsic lattice dynamics driven by strong electron–phonon and phonon–phonon coupling.

The formation of LERs is enabled by the soft and anharmonic lattice of MHPs, which supports hot phonon bottlenecks, localised vibrational modes, and low thermal conductivityfeatures well-documented in recent experimental studies.[133–135] These LERs act as nanoscopic " energy reservoir " capable of storing excess energy from hot carriers and later redistributing it *via* vibrational or vibronic transitions.[113] The LBSC concept, exploits this retained energy to drive phonon-assisted upconversion, forming a feedback loop that recycles waste energy into useful electronic transitions. Notably, the system avoids the need for complex multilayer tandem structures while achieving similar spectral breadth and even lower thermal losses. Theoretical modelling suggests that such architecture could reach efficiencies exceeding 70% under ideal solar conditions, with a potential to capture up to 85% of the incident solar spectrum.[107,113] Beyond efficiency, LBSCs also offer practical advantages: the monolithic structure simplifies manufacturing, and energy recycling reduces heat build-up, which may enhance long-term device stability. These traits position LBSCs not only as a conceptual advance in third-generation photovoltaics but also as a potentially

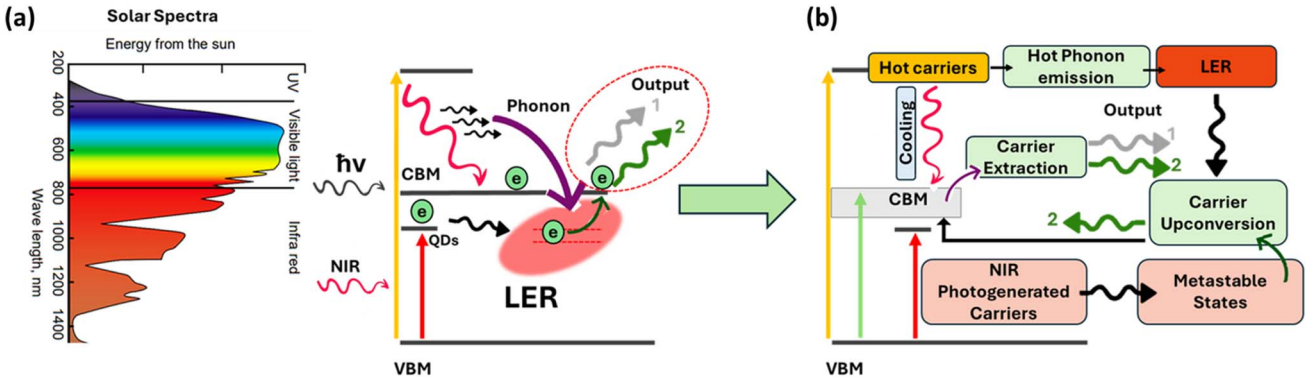

Fig. 6 (a) Establishment of lattice energy reservoir: by phonon-lattice coupling, the energy can gradually accumulate into sublattice/lattice and forming a hot lattice energy reservoir. NIR-photogenerated electron can be controlled for effectively transfer into the metastable state (in-bandgap). These electrons can be upconverted up to the CB of perovskite driven by hot lattice energy reservoir and eventually output as electricity.[107] (b) Energy conversion and output processes in an LBSC under solar emission. LER will save the extra energy from hot carrier and drive NIR-generated in-band carrier upconversion.[107] Adopted from Ghasemi *et al.*, *EcoEnergy*, 2024,[107] published by Wiley, under the terms of the Creative Commons Attribution 4.0 International License (CC BY 4.0).

manufacturable solution that aligns with the 'golden triangle' of solar energy conversion: high performance, low cost, and durability. While experimental realisation remains ongoing, the LBSC embodies the practical application of the LER concept introduced in this review, providing a novel framework to unify photonic and phononic management in halide perovskites.

Future research should aim to validate the presence and dynamics of LERs through time-dependent ultrahigh-spatial resolution characterization techniques; obviously the challenges come from the durability under electron beam of perovskites, high precision detection capability for lattice and strain and repeatable dynamic observation. The LER could redefine the limits of solar energy conversion by introducing a previously unrecognized energy-retention mechanism intrinsic to MHPs. While conventional phonon lifetimes are typically in the picosecond range, coupled lattice-carrier states, such as polarons, can exhibit effective lifetimes ranging from tens to hundreds of picoseconds, and in rare cases, up to nanoseconds under suppressed thermal dissipation. In the context of rare-earth upconversion or phonon recycling systems, persistent lattice excitation has been observed on nanosecond or longer timescales under high excitation densities.[112,136] While direct imaging of LERs remains a challenge, the proposed LER mechanism is supported by several experimental observations in halide perovskites, including anomalous phenomena such as an exceptionally longer[114] carrier recombination lifetime than that predicted by Langevin theory,[115,116] slowed cooling of hot carriers,[117] defect tolerance,[118–120] anomalous upconversion fluorescence (exclusive multi-photon absorption and lanthanum-doping),[121,122] as well as persistent structural polarization,[123] memory,[124,125] and ultraslow variations in photoluminescence (PL) efficiency and carrier lifetime (also referred as to defect healing, defect curing, photobrightening);[126–129] all of which suggest energy retention mechanisms not explained by conventional recombination dynamics. The formation of LERs is linked to strong carrier-lattice coupling and the dynamic strain environment of soft perovskite lattices, which support vibrational bottlenecks and delayed energy redistribution.[136] Studies have also drawn parallels to hot phonon bottlenecks observed in polar semiconductors, where phonon accumulation delays thermalization, especially under continuous excitation.[137] Furthermore, LER-related behaviours, such as nonlinear PL dynamics, persistent spectral shifts, and excitation-dependent carrier recombination, are supported by recent reports from ultrafast spectroscopy and *in situ* PL measurements on MHPs. Future studies should focus on identifying spectral, thermal, or structural fingerprints unique to LER behaviour, such as strain-coupled delayed emission or localized heating signatures, to distinguish it from known defect- or polaron-mediated processes.

4.1. A comparison

The concept of LER presents a fundamentally different mechanism for managing intrinsic solar cell losses compared to previous third-generation strategies such as intermediate bandgap solar cells (IBSCs), hot carrier solar cells (HCSCs), upconversion systems (UCs), downconversion and down-shifting approaches (DC/DS), and tandem solar cells (TSCs). While each of these technologies targets specific energy loss channels, either hot carrier thermalisation or sub-bandgap photon transmission, they often face intrinsic limitations that may be addressed more holistically through LER-enabled energy retention and transfer processes. DC and DS approaches, while often grouped with sub-bandgap photon management, also play a role in reducing thermalisation losses by converting high-energy photons into lower-energy ones better matched to the bandgap, thereby minimising hot carrier generation. Their inclusion here acknowledges the overlap between spectral reshaping strategies and thermal loss mitigation, and reinforces the need for integrated approaches. IBSCs aim to enhance spectral utilization by incorporating an intermediate energy band within the absorber material, enabling sub-bandgap photon absorption *via* sequential two-photon

excitation.[19,138] However, sustaining a stable and well-isolated intermediate state remains inherently challenging due to rapid carrier relaxation and competing nonradiative recombination. Moreover, IBSCs are intrinsically limited to addressing sub-bandgap transmission and do not mitigate hot carrier thermalization. In contrast, the LBSC system offers an integrated mechanism that recycles phonon energy from thermalizing hot carriers and uses it to drive phonon-assisted upconversion of sub-bandgap carriers. This unified energy management strategy conceptually addresses both spectral and thermal losses within a single lattice-coupled system.

Upconversion systems, such as those employing triplet fusion or rare-earth-doped nanoparticles, convert low-energy photons into higher-energy excitations that can be harvested by the solar absorber. However, these approaches typically rely on nonlinear optical processes, demand high excitation intensities, and suffer from limited efficiency under standard solar conditions.[35] In contrast, the LBSC framework introduces a linear, phonon-assisted upconversion pathway wherein dynamically retained lattice energy within nanodomains facilitates the promotion of sub-bandgap carriers to the conduction band. This mechanism bypasses the need for multi-photon absorption and exotic materials, offering a potentially more scalable and efficient route to spectral extension under real-world illumination conditions. HCSCs aim to harvest hot carriers before they lose energy *via* rapid thermalization, theoretically enabling high photovoltages. However, this requires sub-picosecond extraction and sharply energy-selective contacts, which remain formidable fabrication and integration challenges.[44] In contrast, the LER approach circumvents the need for ultrafast extraction by enabling transient retention of excess carrier energy through dynamic coupling with the perovskite lattice. This retained energy can subsequently drive upconversion or delayed excitation pathways, offering a temporally flexible and structurally simpler route to harvesting hot carrier energy.

TSCs achieve high efficiencies by stacking materials with complementary bandgaps to harvest a broader portion of the solar spectrum.[139] Despite their success, TSCs are constrained by complex device architectures, current-matching requirements, and costly multilayer fabrication processes. Moreover, each sub-cell continues to experience intrinsic losses from thermalisation and incomplete sub-bandgap photon utilisation. In contrast, a single-absorber system incorporating LER functionality, introduced here as LBSC, offers a fundamentally distinct strategy that combines hot phonon energy recycling with sub-bandgap carrier activation within a unified, dynamically coupled lattice framework.[107,113,140] This approach does not merely emulate the spectral reach of tandem devices; it proposes an alternative architecture that retains and repurposes otherwise lost energy through intrinsic material physics, offering potential gains without the structural or processing complexities of TSCs. Grounded in the unique vibrational and electronic properties of metal halide perovskites, the LBSC concept represents a transformative avenue toward high-efficiency, single-junction solar energy conversion.

4.2. Advantages of lattice battery solar cell

LBSC grounded in the LER framework, offer a promising strategy to overcome the two principal losses in single-junction photovoltaics: hot carrier thermalisation and sub-bandgap photon loss. By capturing and storing excess phonon energy within vibrationally confined lattice domains, and reusing it to upconvert NIR-excited carriers, LBSCs enable dual-function energy recovery that operates within a single absorber. This integrated approach eliminates the need for complex tandem architectures or non-linear optical schemes, offering a path to high efficiency with structural simplicity. Theoretical predictions indicate that LBSCs could exceed 70% power conversion efficiency under idealised solar illumination, surpassing the Shockley–Queisser limit without resorting to spectral splitting or multi-junction designs.[107,113] In parallel, the energy retention characteristics of LERs may contribute to thermal stability by redistributing carrier energy rather than dissipating it as heat, a known degradation trigger in perovskite devices. By mitigating thermal load at the lattice level, LBSCs hold promise for improved operational lifetimes. Furthermore, LBSCs retain the scalable and cost-effective processing routes of conventional perovskite single-junction solar cells. Their compatibility with solution-based fabrication and absence of stringent current-matching constraints make them particularly well-suited to low-cost manufacturing. By simultaneously addressing efficiency, stability, and processability-the "golden triangle" of solar energy technology-LBSCs present a compelling design paradigm for the next generation of high-performance photovoltaics.

5. Summary and outlook

In response to the limitations of current solar cell technologies, there is a growing imperative to explore novel photovoltaic concepts capable of overcoming long-standing theoretical efficiency ceilings. The pursuit of next-generation solar energy conversion has led to the emergence of third-generation technologies that promise flexibility, lightweight design, cost-effectiveness, and improved efficiencies. Among these, significant attention has been given to alternative materials, such as organic semiconductors, polymers, and halide perovskites, as well as advanced architectures including two-terminal tandem solar cells. Tandem cells have demonstrated strong potential, with theoretical power PCEs approaching 50%. Similarly, carrier multiplication (CM) and hot carrier (HC) extraction strategies aim to reduce thermal losses, offering theoretical efficiency ceilings around 44% and 67%, respectively. Despite these compelling theoretical prospects, most of these advanced strategies remain at a conceptual or laboratory stage. Persistent challenges, such as material integration complexity, thermal instability, limited scalability, and cost, have limited their practical deployment. Bridging the gap between these innovative ideas and real-world application remains a central challenge in photovoltaic research. In this landscape, MHPs have emerged as a transformative class of materials. Their exceptional defect tolerance, efficient charge transport, and tuneable

optoelectronic properties enable impressive efficiencies of 25–30% in single-junction architectures. These intrinsic qualities have made MHPs a fertile ground for exploring unconventional mechanisms of solar energy conversion.

One such mechanism is the recently proposed concept of the LER, a hypothesized metastable nanodomain within the MHP lattice that can capture and temporarily store phonon energy generated by hot carriers. Unlike conventional semiconductors where excess energy is lost to rapid thermalization, MHPs exhibit ultraslow energy dissipation processes that may support such energy-retaining structures. While the LER remains an unconfirmed phenomenon, its theoretical foundation is supported by a range of anomalous behaviours observed in perovskites, including photobrightening, hysteresis, phase segregation, and ultralow thermal conductivity. If experimentally validated, the LER could provide a novel pathway for energy recycling within a solar absorber. It may enable phonon-driven upconversion of sub-bandgap carriers and offer a solution to both thermalization and non-absorption losses, two of the most significant limitations defined by the Shockley–Queisser model. Building on this foundation, the concept of LBSCs has been introduced as a hypothetical device architecture that utilizes the LER to enhance energy harvesting within a single-junction structure. LBSCs aim to integrate spectral broadening and energy retention within one material system, leveraging the inherent properties of MHPs to enable high efficiency, operational stability, and cost-effective fabrication. While still in the theoretical stage, the LBSC concept illustrates the type of innovative thinking required to push beyond conventional solar cell design paradigms.

The ongoing exploration of MHPs and their dynamic lattice behaviour opens exciting new directions in photovoltaic research. The LER represents a promising, albeit unproven, mechanism that could redefine how energy is captured, retained, and converted in solar cells. LBSCs, as a conceptual framework inspired by LER, exemplify how foundational material physics can lead to radically new device possibilities. Further experimental work is now essential to investigate the validity and potential of LERs, paving the way for future technologies that may one day exceed current theoretical efficiency limits and contribute meaningfully to global renewable energy goals.

Data availability

The data supporting this article has been included in the manuscript.

Conflicts of interest

The authors declare that they have no conflict of interest.

Acknowledgements

Authors acknowledge financial support from Australian Research Council FT210100806, DP220100603, CE230100006, LP240100504.

References

1 M. Green, E. Dunlop, J. Hohl-Ebinger, M. Yoshita, N. Kopidakis and X. Hao, *Prog. Photovolt.: Res. Appl.*, 2021, **29**, 3–15.
2 A. Sadiqa, A. Gulagi, D. Bogdanov, U. Caldera and C. Breyer, *IET Renew. Power Gener.*, 2022, **16**, 177–197.
3 A. Sadiqa, A. Gulagi, D. Bogdanov, U. Caldera and C. Breyer, *IET Renew. Power Gener.*, 2022, **16**, 177–197.
4 M. A. Green, *Prog. Photovolt.: Res. Appl.*, 2001, **9**, 123–135.
5 S. Bhattacharya and S. John, *Sci. Rep.*, 2019, **9**, 12482.
6 A. Le Donne, V. Trifiletti and S. Binetti, *Front. Chem.*, 2019, **7**, 297.
7 J. Ramanujam, D. M. Bishop, T. K. Todorov, O. Gunawan, J. Rath, R. Nekovei, E. Artegiani and A. Romeo, *Prog. Mater. Sci.*, 2020, **110**, 100619.
8 P. Meredith and A. Armin, *Nat. Commun.*, 2018, **9**, 5261.
9 K. Jayawardena, S. Silva and R. Misra, *J. Mater. Chem. C*, 2020, **8**, 10641–10675.
10 M. A. Green, *Third Generation Photovoltaics: Advanced Solar Energy Conversion*, Springer Series in Photonics, Springer, Berlin, Heidelberg, 2003, vol. 12, ISBN: 978-3-540-00551-0, DOI: 10.1007/b137807.
11 M. A. Green, *Prog. Photovolt.: Res. Appl.*, 2000, **9**, 123–135.
12 W. Shockley and H. Queisser, in *Renewable Energy*, Routledge, 2018, pp. 35–54.
13 A. Luque and A. Martí, *Phys. Rev. Lett.*, 1997, **78**, 5014.
14 I. Ramiro, A. Martí, E. Antolin and A. Luque, *IEEE J. Photovolt.*, 2014, **4**, 736–748.
15 J. An, H. Jiang, Y. Tian, H. Xue and F. Tang, *Phys. Chem. Chem. Phys.*, 2019, **21**, 23552–23558.
16 M. Sampson, J. Park, R. Schaller, M. Chan and A. Martinson, *J. Mater. Chem. A*, 2017, **5**, 3578–3588.
17 M. Rasukkannu, D. Velauthapillai and P. Vajeeston, *Mater. Lett.*, 2018, **218**, 233–236.
18 X. Ma and Z. Li, *Phys. Chem. Chem. Phys.*, 2020, **22**, 23804–23809.
19 H. Hosokawa, R. Tamaki, T. Sawada, A. Okonogi, H. Sato, Y. Ogomi, S. Hayase, Y. Okada and T. Yano, *Nat. Commun.*, 2019, **10**, 43.
20 W. Zheng, P. Huang, Z. Gong, D. Tu, J. Xu, Q. Zou, R. Li, W. You, J.-C. G. Bünzli and X. Chen, *Nat. Commun.*, 2018, **9**, 3462.
21 S. Zheng, J. Chen, E. M. J. Johansson and X. Zhang, *iScience*, 2020, **23**, 101753.
22 M. Amjad, M. Khan, N. Alwadai and M. Irfan, *Nanomaterials*, 2022, **12**, 1057.
23 M. Cirignano, *Energy Fuels*, 2024, **35**, 18928–18941; *Chem. Rev.*, 2023, **123**, 3625–3692.
24 A. Martí and A. Luque, *Next Generation Photovoltaics: High Efficiency through Full Spectrum Utilization*, CRC Press, 2003.
25 T. N. Singh-Rachford and F. N. Castellano, *Coord. Chem. Rev.*, 2010, **254**, 2560–2573.
26 D. H. Weingarten, M. D. LaCount, J. van de Lagemaat, G. Rumbles, M. T. Lusk and S. E. Shaheen, *Nat. Commun.*, 2017, **8**, 14808.

27 J. Moffatt, G. Tsiminis, E. Klantsataya, T. de Prinse, D. Ottaway and N. Spooner, *Appl. Spectrosc. Rev.*, 2020, **55**, 327–349.
28 H. Ye, V. Bogdanov, S. Liu, S. Vajandar, T. Osipowicz, I. Hernandez and Q. Xiong, *J. Phys. Chem. Lett.*, 2017, **8**, 5695–5699.
29 J. Wang, T. Ming, Z. Jin, J. Wang, L.-D. Sun and C.-H. Yan, *Nat. Commun.*, 2014, **5**, 5669.
30 N. Bloembergen, *Phys. Rev. Lett.*, 1959, **2**, 84.
31 J. C. Goldschmidt and S. Fischer, *Adv. Opt. Mater.*, 2015, **3**, 510–535.
32 X. Guo, W. Wu, Y. Li, J. Zhang, L. Wang and H. Ågren, *Chin. Chem. Lett.*, 2021, **32**, 1834–1846.
33 S. Fischer, A. Ivaturi, P. Jakob, K. W. Krämer, R. Martin-Rodriguez, A. Meijerink, B. Richards and J. C. Goldschmidt, *Opt. Mater.*, 2018, **84**, 389–395.
34 G. A. Nowsherwan, M. Khan, N. Nowsherwan, S. Ikram, S. S. Hussain, S. Naseem and S. Riaz, *J. Mater. Sci.*, 2024, **59**, 16411–16448.
35 Y. Shang, S. Hao, C. Yang and G. Chen, *Nanomaterials*, 2015, **5**, 1782–1809.
36 J. de Wild, A. Meijerink, J. Rath, W. Van Sark and R. Schropp, *Energy Environ. Sci.*, 2011, **4**, 4835–4848.
37 Y. Yang, D. P. Ostrowski, R. M. France, K. Zhu, J. Van De Lagemaat, J. M. Luther and M. C. Beard, *Nat. Photonics*, 2016, **10**, 53–59.
38 F. Chen, A. Cartwright, H. Lu and W. J. Schaff, *Appl. Phys. Lett.*, 2003, **83**, 4984–4986.
39 S. A. Bretschneider, F. Laquai and M. Bonn, *J. Phys. Chem. C.*, 2017, **121**, 11201–11206.
40 H.-H. Fang, S. Adjokatse, S. Shao, J. Even and M. A. Loi, *Nat. Commun.*, 2018, **9**, 243.
41 X. Jia, J. Jiang, Y. Zhang, J. Qiu, S. Wang, Z. Chen, N. Yuan and J. Ding, *Appl. Phys. Lett.*, 2018, **112**, 143903.
42 R. T. Ross and A. J. Nozik, *J. Appl. Phys.*, 1982, **53**, 3813–3818.
43 D. König, K. Casalenuovo, Y. Takeda, G. Conibeer, J. F. Guillemoles, R. Patterson, L. M. Huang and M. A. Green, *Physica E Low Dimens. Syst. Nanostruct.*, 2010, **42**, 2862–2866.
44 W. Lin, S. E. Canton, K. Zheng and T. Pullerits, *ACS Energy Lett.*, 2024, **9**, 298–307.
45 A. Le Bris, L. Lombez, S. Laribi, G. Boissier, P. Christol and J.-F. Guillemoles, *Energy Environ. Sci.*, 2012, **5**, 6225–6232.
46 S. K. Shrestha, P. Aliberti and G. J. Conibeer, *Sol. Energy Mater. Sol. Cells*, 2010, **94**, 1546–1550.
47 Y. Chen, Y. Li, Y. Zhao, H. Zhou and H. Zhu, *Sci. Adv.*, 2019, **5**, eaax9958.
48 M. Massicotte, G. Soavi, A. Principi and K.-J. Tielrooij, *Nanoscale*, 2021, **13**, 8376–8411.
49 K. K. Paul, J.-H. Kim and Y. H. Lee, *Nat. Rev. Phys.*, 2021, **3**, 178–192.
50 L. Xu, W.-Q. Huang, W. Hu, K. Yang, B.-X. Zhou, A. Pan and G.-F. Huang, *Chem. Mater.*, 2017, **29**, 5504–5512.
51 N. Siemons and A. Serafini, *J. Nanotechnol.*, 2018, **2018**, 7285483.
52 L. Tesser, R. S. Whitney and J. Splettstoesser, *Phys. Rev. Appl.*, 2023, **19**, 044038.
53 Y. Takeda, in *Quantum & Nano Technologies for Photovoltaics*, CRC Press, 2019, pp. 81–120.
54 A. J. Nozik, *Chem. Phys. Lett.*, 2008, **457**, 3–11.
55 P. Landsberg, H. Nussbaumer and G. Willeke, *J. Appl. Phys.*, 1993, **74**, 1451–1452.
56 O. E. Semonin, J. M. Luther, S. Choi, H.-Y. Chen, J. Gao, A. J. Nozik and M. C. Beard, *Science*, 2011, **334**, 1530–1533.
57 M. Li, R. Begum, J. Fu, Q. Xu, T. M. Koh, S. A. Veldhuis, M. Grätzel, N. Mathews, S. Mhaisalkar and T. C. Sum, *Nat. Commun.*, 2018, **9**, 4197.
58 K. Hyeon-Deuk and O. V. Prezhdo, *ACS Nano*, 2012, **6**, 1239–1250.
59 C. de Weerd, L. Gomez, A. Capretti, D. M. Lebrun, E. Matsubara, J. Lin, M. Ashida, F. C. Spoor, L. D. Siebbeles and A. J. Houtepen, *Nat. Commun.*, 2018, **9**, 4199.
60 M. C. Beard, A. G. Midgett, M. C. Hanna, J. M. Luther, B. K. Hughes and A. J. Nozik, *Nano Lett.*, 2010, **10**, 3019–3027.
61 M. C. Beard and R. J. Ellingson, *Laser Photonics Rev.*, 2008, **2**, 377–399.
62 C. J. Stolle, T. B. Harvey, D. R. Pernik, J. I. Hibbert, J. Du, D. J. Rhee, V. A. Akhavan, R. D. Schaller and B. A. Korgel, *J. Phys. Chem. Lett.*, 2014, **5**, 304–309.
63 D. Boudreaux, F. Williams and A. Nozik, *J. Appl. Phys.*, 1980, **51**, 2158–2163.
64 A. J. Nozik, in *Next Generation of Photovoltaics: New Concepts*, Springer, 2012, pp. 191–207.
65 S. Tomić, J. M. Miloszewski, E. J. Tyrrell and D. J. Binks, *IEEE J. Photovolt.*, 2015, **6**, 179–184.
66 T. Luo, Y. Zhang, Z. Xu, T. Niu, J. Wen, J. Lu, S. Jin, S. Liu and K. Zhao, *Adv. Mater.*, 2019, **31**, 1903848.
67 M. Ghasemi, B. Jia and X. Wen, *EcoEnergy*, 2024, **2**, 448–455.
68 S. Sahu, S. Khan, A. Tripathy, K. Dey, N. Bano, S. Raj Mohan, M. Joshi, S. Verma, B. Rao and V. Sathe, *Phys. Rev. B*, 2023, **108**, 125133.
69 P. Zhang, Y. Wang, X. Su, Q. Zhang and M. Sun, *Nanomaterials*, 2024, **14**, 558.
70 Z. Ding, S. Li, Y. Jiang, D. Wang and M. Yuan, *Nanoscale*, 2023, **15**, 3713–3729.
71 H. Huang, X. Zhang, C. Zhao and J. Yuan, *Mater. Chem. Front.*, 2023, **7**, 1423–1430.
72 N. J. Thompson, D. N. Congreve, D. Goldberg, V. M. Menon and M. A. Baldo, *Appl. Phys. Lett.*, 2013, **103**, 263302.
73 L. Yang, M. Tabachnyk, S. L. Bayliss, M. L. Böhm, K. Broch, N. C. Greenham, R. H. Friend and B. Ehrler, *Nano Lett.*, 2015, **15**, 354–358.
74 L. M. Pazos-Outón, J. M. Lee, M. H. Futscher, A. Kirch, M. Tabachnyk, R. H. Friend and B. Ehrler, *ACS Energy Lett.*, 2017, **2**, 476–480.
75 D. López-Carballeira and T. Polcar, *ChemPhotoChem*, 2023, **7**, e202300017.
76 T. Wang, H. Liu, X. Wang, L. Tang, J. Zhou, X. Song, L. Lv, W. Chen, Y. Chen and X. Li, *J. Mater. Chem. A*, 2023, **11**, 8515–8539.

77 D. N. Congreve, J. Lee, N. J. Thompson, E. Hontz, S. R. Yost, P. D. Reusswig, M. E. Bahlke, S. Reineke, T. Van Voorhis and M. A. Baldo, *Science*, 2013, **340**, 334–337.
78 A. D. Vos, *J. Phys. D: Appl. Phys.*, 1980, **13**, 839.
79 H. Li and W. Zhang, *Chem. Rev.*, 2020, **120**, 9835–9950.
80 T. Leijtens, K. A. Bush, R. Prasanna and M. D. McGehee, *Nat. Energy*, 2018, **3**, 828–838.
81 P. Gnida, M. F. Amin, A. K. Pająk and B. Jarząbek, *Polymers*, 2022, **14**, 1946.
82 J. You, L. Dou, K. Yoshimura, T. Kato, K. Ohya, T. Moriarty, K. Emery, C.-C. Chen, J. Gao, G. Li and Y. Yang, *Nat. Commun.*, 2013, **4**, 1446.
83 L. Meng, Y. Zhang, X. Wan, C. Li, X. Zhang, Y. Wang, X. Ke, Z. Xiao, L. Ding, R. Xia, H.-L. Yip, Y. Cao and Y. Chen, *Science*, 2018, **361**, 1094–1098.
84 S. Saravanan, R. Kato, M. Balamurugan, S. Kaushik and T. Soga, *J. Sci.:Adv. Mater. Devices*, 2017, **2**, 418–424.
85 B. Chen, S.-W. Baek, Y. Hou, E. Aydin, M. De Bastiani, B. Scheffel, A. Proppe, Z. Huang, M. Wei, Y.-K. Wang, E.-H. Jung, T. G. Allen, E. Van Kerschaver, F. P. García de Arquer, M. I. Saidaminov, S. Hoogland, S. De Wolf and E. H. Sargent, *Nat. Commun.*, 2020, **11**, 1257.
86 E. Lamanna, F. Matteocci, E. Calabrò, L. Serenelli, E. Salza, L. Martini, F. Menchini, M. Izzi, A. Agresti and S. Pescetelli, *Joule*, 2020, **4**, 865–881.
87 J. Xu, C. C. Boyd, Z. J. Yu, A. F. Palmstrom, D. J. Witter, B. W. Larson, R. M. France, J. Werner, S. P. Harvey, E. J. Wolf, W. Weigand, S. Manzoor, M. F. A. M. van Hest, J. J. Berry, J. M. Luther, Z. C. Holman and M. D. McGehee, *Science*, 2020, **367**, 1097–1104.
88 B. Chen, N. Ren, Y. Li, L. Yan, S. Mazumdar, Y. Zhao and X. Zhang, *Adv. Energy Mater.*, 2022, **12**, 2003628.
89 T. Leijtens, G. E. Eperon, N. K. Noel, S. N. Habisreutinger, A. Petrozza and H. J. Snaith, *Adv. Energy Mater.*, 2015, **5**, 1500963.
90 H. Cho, Y. H. Kim, C. Wolf, H. D. Lee and T. W. Lee, *Adv. Mater.*, 2018, **30**, 1704587.
91 L. Kong, X. Zhang, C. Zhang, L. Wang, S. Wang, F. Cao, D. Zhao, A. L. Rogach and X. Yang, *Adv. Mater.*, 2022, **34**, 2205217.
92 W. Xiang, S. F. Liu and W. Tress, *Energy Environ. Sci.*, 2021, **14**, 2090–2113.
93 L. Duan, D. Walter, N. Chang, J. Bullock, D. Kang, S. P. Phang, K. Weber, T. White, D. Macdonald and K. Catchpole, *Nat. Rev. Mater.*, 2023, **8**, 261–281.
94 J. Liu, Y. He, L. Ding, H. Zhang, Q. Li, L. Jia, J. Yu, T. W. Lau, M. Li and Y. Qin, *Nature*, 2024, **635**, 596–603.
95 F. Zhang, B. Tu, S. Yang, K. Fan, Z. Liu, Z. Xiong, J. Zhang, W. Li, H. Huang and C. Yu, *Adv. Mater.*, 2023, **35**, 2303139.
96 A. S. Subbiah, F. H. Isikgor, C. T. Howells, M. De Bastiani, J. Liu, E. Aydin, F. Furlan, T. G. Allen, F. Xu and S. Zhumagali, *ACS Energy Lett.*, 2020, **5**, 3034–3040.
97 K. Xu, A. Al-Ashouri, Z.-W. Peng, E. Köhnen, H. Hempel, F. Akhundova, J. A. Marquez, P. Tockhorn, O. Shargaieva and F. Ruske, *ACS Energy Lett.*, 2022, **7**, 3600–3611.
98 D. L. Dexter, *Phys. Rev.*, 1957, **108**, 630–633.
99 N. S. Satpute, C. M. Mehare, A. Tiwari, H. C. Swart and S. J. Dhoble, *ACS Appl. Electron. Mater.*, 2022, **4**, 3354–3391.
100 H. Lian, Z. Hou, M. Shang, D. Geng, Y. Zhang and J. Lin, *Energy*, 2013, **57**, 270–283.
101 V. Balaram, *Geosci Front.*, 2019, **10**, 1285–1303.
102 R. Nölle, K. Beltrop, F. Holtstiege, J. Kasnatscheew, T. Placke and M. Winter, *Mater. Today*, 2020, **32**, 131–146.
103 M. L. Scherff, J. Nutter, P. Fuss-Kailuweit, J. Suthues and T. Brammer, *Jpn. J. Appl. Phys.*, 2017, **56**, 08MB24.
104 F. Schubert and D. Spinner, *Energy Procedia*, 2016, **92**, 205–210.
105 T. Song, T. Moriarty and D. Levi, 2019.
106 M. P. Belançon, M. Sandrini, V. S. Zanuto and R. F. Muniz, *J. Non-Cryst. Solids*, 2023, **619**, 122548.
107 M. Ghasemi, B. Jia and X. Wen, *EcoEnergy*, 2024, **2**, 448–455.
108 G. Liu, M. Ghasemi, Q. Wei, B. Jia, Y. Yang and X. Wen, *Adv. Energy Mater.*, 2025, **15**, 2405239.
109 G. Liu, Q. Wei, G. Zhang, M. Ghasemi, q. Li, J. Lu, J. Wang, B. Jia, Y. Yu and X. Wen, *J. Mater. Chem. C*, 2024, **12**, 8309–8319.
110 G. Zhang, Q. Wei, G. Liu, Q. Li, J. Lu, M. Ghasemi, J. Wang, Y. Yang, B. Jia and X. Wen, *ACS Appl. Mater. Interfaces*, 2024, **16**, 14263–14274.
111 G. Zhang, Q. Wei, M. Ghasemi, G. Liu, J. Wang, B. Zhou, J. Luo, Y. Yang, B. Jia and X. Wen, *Small Sci.*, 2024, **4**, 2400028.
112 J. Lu, Z. Gan, J. van Embden, B. Jia and X. Wen, *Mater. Today*, 2025, **86**, 340–355.
113 M. Ghasemi, D. Lan, B. Jia and X. Wen, *Innov. Energy.*, 2025, **2**, 100091–100092.
114 Z. Andaji-Garmaroudi, M. Anaya, A. J. Pearson and S. D. Stranks, *Adv. Energy Mater.*, 2020, **10**, 1903109.
115 M. B. Johnston and L. M. Herz, *Acc. Chem. Res.*, 2016, **49**, 146–154.
116 J. Van Der Holst, F. Van Oost, R. Coehoorn and P. Bobbert, *Phys. Rev. B:Condens. Matter Mater. Phys.*, 2009, **80**, 235202.
117 D. W. Dequilettes, K. Frohna, D. Emin, T. Kirchartz, V. Bulovic, D. S. Ginger and S. D. Stranks, *Chem. Rev.*, 2019, **119**, 11007–11019.
118 J. Kang and L.-W. Wang, *J. Phys. Chem. Lett.*, 2017, **8**, 489–493.
119 G. W. Kim and A. Petrozza, *Adv. Energy Mater.*, 2020, **10**, 2001959.
120 G. Liu, Q. Wei, G. Zhang, M. Ghasemi, Q. Li, J. Lu, J. Wang, B. Jia, Y. Yang and X. Wen, *J. Mater. Chem. C*, 2024, **12**, 8309–8319.
121 A. Granados del Águila, T. T. H. Do, J. Xing, W. J. Jee, J. B. Khurgin and Q. Xiong, *Nano Res.*, 2020, **13**, 1962–1969.
122 Z. Zhang, S. Ghonge, Y. Ding, S. Zhang, M. Berciu, R. D. Schaller, B. Jankó and M. Kuno, *ACS Nano*, 2024, **18**, 6438–6444.
123 Q. Qian, Z. Wan, H. Takenaka, J. K. Keum, T. J. Smart, L. Wang, P. Wang, J. Zhou, H. Ren, D. Xu, Y. Huang, Y. Ping and X. Duan, *Nat. Nanotechnol.*, 2023, **18**, 357–364.
124 K. Kang, H. Ahn, Y. Song, W. Lee, J. Kim, Y. Kim, D. Yoo and T. Lee, *Adv. Mater.*, 2019, **31**, 1804841.

125 J. Di, J. Du, Z. Lin, S. Liu, J. Ouyang and J. Chang, *InfoMat*, 2021, **3**, 293–315.
126 Y. Tian, M. Peter, E. Unger, M. Abdellah, K. Zheng, T. Pullerits, A. Yartsev, V. Sundström and I. G. Scheblykin, *Phys. Chem. Chem. Phys.*, 2015, **17**, 24978–24987.
127 S. Ghosh, Q. Shi, B. Pradhan, A. Mushtaq, S. Acharya, K. J. Karki, T. Pullerits and S. K. Pal, *J. Phys. Chem. Lett.*, 2020, **11**, 1239–1246.
128 W. Nie, J.-C. Blancon, A. J. Neukirch, K. Appavoo, H. Tsai, M. Chhowalla, M. A. Alam, M. Y. Sfeir, C. Katan and J. Even, *Nat. Commun.*, 2016, **7**, 11574.
129 S. Chen, X. Wen, S. Huang, F. Huang, Y. B. Cheng, M. Green and A. Ho-Baillie, *Solar Rrl*, 2017, **1**, 1600001.
130 Y. Yuan, G. Yan, C. Dreessen, T. Rudolph, M. Hülsbeck, B. Klingebiel, J. Ye, U. Rau and T. Kirchartz, *Nat. Mater.*, 2024, **23**, 391–397.
131 L. Yang, S. Yue, Y. Tao, S. Qiao, H. Li, Z. Dai, B. Song, Y. Chen, J. Du and D. Li, *Nature*, 2024, **629**, 1021–1026.
132 M. Wang and S. Lin, *Adv. Funct. Mater.*, 2016, **26**, 5297–5306.
133 Z. Guo, J. Wang and W.-J. Yin, *Energy Enviro. Sci.*, 2022, **15**, 660–671.
134 R. Heiderhoff, T. Haeger, N. Pourdavoud, T. Hu, M. Al-Khafaji, A. Mayer, Y. Chen, H.-C. Scheer and T. Riedl, *J. Phys. Chem. C.*, 2017, **121**, 28306–28311.
135 Y. Wang, R. Lin, P. Zhu, Q. Zheng, Q. Wang, D. Li and J. Zhu, *Nano Lett.*, 2018, **18**, 2772–2779.
136 X. Wen and B. Jia, *Acc. Mater. Res.*, 2025, DOI: **10.1021/accountsmr.5c00047**.
137 J. Yang, X. Wen, H. Xia, R. Sheng, Q. Ma, J. Kim, P. Tapping, T. Harada, T. W. Kee and F. Huang, *Nat. Commun.*, 2017, **8**, 14120.
138 S. Tomić, *Phys. Rev. B:Condens. Matter Mater. Phys.*, 2010, **82**, 195321.
139 Q. Wali, N. K. Elumalai, Y. Iqbal, A. Uddin and R. Jose, *Renewable Sustainable Energy Rev.*, 2018, **84**, 89–110.
140 B. J. Junlin lu and X. Wen, *Materials Today*, In Press, 2025.